

Diffusion and segregation of silver in copper $\Sigma 5(310)$ grain boundary

Sergiy V. Divinski* and Henning Edelhoff

Institute of Materials Physics, University of Münster, Wilhelm-Klemm-Str. 10, D-48149 Münster, Germany

Sergei Prokofjev

Institute of Solid State Physics, Chernogolovka, 142432 Moscow Region, Russia

(Received 27 January 2012; revised manuscript received 15 March 2012; published 6 April 2012)

Grain boundary diffusion of ^{110m}Ag in Cu $\Sigma 5(310)$ bicrystal is measured along and perpendicular to the [001] tilt axis in both C and B kinetic regimes after the common Harrison's classification. The grain boundary diffusion coefficients, D_{gb} , of the *single grain boundary* in a true dilute limit of solute concentration are determined in the C kinetic regime and the values of the triple products $P = s \cdot \delta \cdot D_{\text{gb}}$ are measured in the B regime (here s and δ are the segregation factor and the diffusional grain boundary width, respectively). A strong anisotropy of the grain boundary diffusion is established, which disappears above 826 K. It is the point at which the triple product P demonstrates a downward deviation from the otherwise linear Arrhenius dependence at lower temperatures. These results substantiate a temperature-induced disordering transition of the grain boundary structure. The anisotropy of the product $s \cdot \delta$ for the $\Sigma 5(310)$ grain boundary is estimated.

DOI: [10.1103/PhysRevB.85.144104](https://doi.org/10.1103/PhysRevB.85.144104)

PACS number(s): 66.30.-h, 68.35.Fx, 68.35.Dv, 61.72.Mm

I. INTRODUCTION

Grain boundary (GB) diffusion represents a unique tool for investigation of the GB kinetic and thermodynamic properties. For example, GB segregation of solutes can reliably be examined both for the dilute, Henry limit and for the nonlinear segregation conditions.¹ The key point is the combination of the C- and B-type measurements after Harrison's classification² in *the same* material. While solely the triple product $P = s \cdot \delta \cdot D_{\text{gb}}$ can be determined in the B regime, C-type experiments provide directly the GB diffusion coefficient D_{gb} .³ Here s and δ are the solute segregation factor and the GB width, respectively. Having measured the values of P and D_{gb} for the same material, the product of the GB segregation factor s and the GB diffusional width δ can be determined:

$$s \cdot \delta = \frac{P}{D_{\text{gb}}}. \quad (1)$$

Then, if δ is known (see below), the solute segregation factor s will be obtained. The main assumptions and limitations of this method as well as recent advances are reviewed, e.g., in Refs. 1 and 4. These GB characteristics are influenced by the chemistry and energy of GBs and determine the kinetics of interface-related processes and, thus, affect many important properties and stability of alloys, especially in fine-grained and nanocrystalline materials.⁵

Having applied this method to a polycrystalline material, the diffusion and segregation properties of general (random) high-angle grain boundaries will be determined. This is explained by the fact that these are the general high-angle GBs which typically provide the fastest short-circuit paths in a (well-annealed) polycrystalline material and govern the atomic transport. While such data are extremely important for technological applications, there is a fundamental need for determination of the diffusion and segregation characteristics of model grain boundaries in order to develop a basic knowledge of the structure-property interrelation for interfaces in a polycrystalline solid. Detailed and systematic

measurements of GB diffusion in well-characterized bicrystals contribute to this goal and a large number of such experiments have been performed so far; see, e.g., the comprehensive reviews in Refs. 3 and 6. However, all those measurements were exclusively carried out under B-type kinetic conditions, whereas C-type experiments were thought to be impossible for bicrystals due to the need to determine the tiny amounts of tracer atoms located solely in the interface of the thickness δ .

To the authors' knowledge, there exists only one series of experimental studies of C-type measurements in bicrystals, namely, Ma and Balluffi⁷ investigated the chemical diffusion of Ag along the misorientation axis of [001] symmetric tilt boundaries in Au thin films by the surface accumulation method, and the parameter $s \cdot \delta \cdot D_{\text{gb}}/s_s$ was determined. Here s_s is the corresponding surface segregation factor. Thus direct data on D_{gb} for single and completely characterized GBs are absent.

Very recently, we succeeded in measuring the solute (Ag) GB diffusion coefficient, D_{gb} , for a single GB in a model Cu $\Sigma 5(310)$ bicrystal.⁸ In the present paper, those measurements are combined with B-type experiments on *the same* bicrystal. The Ag diffusion is determined both parallel and perpendicular to the [001] tilt axis and the anisotropy of both P and D_{gb} , and thus of the product $s \cdot \delta$, is evaluated for a single and precisely characterized GB for the first time.

II. EXPERIMENTAL DETAILS**A. Materials**

A bicrystal with dimensions of $6 \times 20 \times 200 \text{ mm}^3$ containing a $\Sigma 5(310)$ GB was grown using a high-purity copper (5N8) from precisely oriented seeds in a high-purity graphite container in an atmosphere of purified argon by a slightly inclined scheme of the Bridgman method. The misorientation between the two crystals is characterized by the main tilt angle, $\theta = (36.3 \pm 0.06)^\circ$, as well as by the "second tilt" angle $\Psi = (1.1 \pm 0.06)^\circ$ and the twist angle $\Phi = (0.3 \pm 0.06)^\circ$. Further details on the bicrystal preparation are given in Ref. 8.

TABLE I. Experimental parameters of GB diffusion measurements in the Cu $\Sigma 5(310)$ bicrystal. T is the diffusion temperature, t the diffusion time, and D_{gb} and P the determined diffusivities. $\alpha^* = \delta/2\sqrt{D_{\text{gb}}t} = \alpha/s$. α and β are the diffusion parameters; see text. The diffusion direction is referred to the [001] main tilt axis of the bicrystal. k_{B} and k_{C} are the correction factors for the diffusivities measured in the transition regime between the C and the B kinetics; see text. The estimated uncertainties in the values of P and D_{gb} do not exceed 15%. A is the diffusion anisotropy and $A = P_{\parallel}/P_{\perp}$ for the B regime and $A = D_{\text{gb}}^{\parallel}/D_{\text{gb}}^{\perp}$ for the C-type measurements. At $T = 675$ K the average value of A is given.

T (K)	t (10^4 s)	Diffusion direction	α^*	β	Regime	D_{gb} (m^2/s)	P (m^3/s)	$s \cdot \delta$ (m)	α	k_{C}	k_{B}	A
534 ^a	121	∥	9.4×10^{-2}	–	C	8.97×10^{-16}	–	1.1×10^{-6}	205	–	–	3.0
		⊥				3.00×10^{-16}	–	1.5×10^{-6}	283			
555 ^a	121	∥	4.1×10^{-2}	–	C	1.98×10^{-15}	–	8.8×10^{-7}	72	–	–	1.4
		⊥				1.43×10^{-15}	–	6.0×10^{-7}	49			
575 ^a	121	∥	2.0×10^{-2}	–	C	4.71×10^{-15}	–	6.1×10^{-7}	24	–	–	3.1
		⊥				1.53×10^{-15}	–	9.8×10^{-7}	39			
675	25.9	∥	2.1×10^{-3}	1.8×10^6	Transition	3.80×10^{-14}	1.32×10^{-20}	2.9×10^{-7}	1.2	2.05	1.76	1.5
		⊥		1.3×10^6		2.90×10^{-14}	7.25×10^{-21}	3.2×10^{-7}	1.3	1.63	2.29	
723	8.65	∥	1.2×10^{-3}	2.1×10^5	Transition	–	3.93×10^{-20}	–	0.47	–	1.27	1.6
		⊥		1.3×10^5		–	2.01×10^{-20}	–	0.52	1.56		
826	7.32	∥	1.7×10^{-4}	2.2×10^3	B	–	2.05×10^{-19}	–	0.038	–	–	1.1
		⊥		1.9×10^3		–	1.80×10^{-19}	–	0.042	–		
923	8.09	∥	3.6×10^{-5}	32	B	–	2.70×10^{-19}	–	5.4×10^{-3}	–	–	1.0
		⊥		31		–	2.61×10^{-19}	–	5.8×10^{-3}	–		

^aThese measurements were performed in Ref. 8 and they are used here for self-consistent determination of the values of $s \cdot \delta$ and α ; see text.

Two kinds of disk-shaped specimens were cut from the bicrystal by spark erosion with the basis planes normal and parallel to the [001] misorientation axis. The specimens were gently polished to a mirror-like finish and subjected to preannealing heat treatment under purified Ar at the temperatures and for the intended times of the subsequent diffusion experiments in order to approach equilibrium segregation conditions for residual impurities.

B. Radiotracer measurements

The $^{110\text{m}}\text{Ag}$ radioisotope (half-life of 252 days) with an initial specific activity of 47.7 MBq/mg was produced by neutron irradiation of a natural silver chip at the research reactor GKSS, Geesthacht, Germany. The activated chip was first dissolved in 20 μl of HNO_3 and further dissolved in 20 ml of double-distilled water in order to reach a specific activity of about 1 kBq/ μl . A droplet of the highly diluted $^{110\text{m}}\text{Ag}$ solution was deposited onto the polished surface of each specimen and dried. The specimens were evacuated in silica ampoules to a residual pressure of less than 10^{-4} Pa, sealed, and annealed.

The temperatures T and times t of the annealing treatments are listed in Table I. After annealing treatment, the samples were reduced in diameter to remove the effect of lateral and/or surface diffusion. The two samples for investigation of diffusion along and perpendicular to the misorientation axis were annealed together to allow direct comparison of the measured diffusivities.

The penetration profiles of $^{110\text{m}}\text{Ag}$ were determined by the serial sectioning technique using an SM2500E microtome (Leica). The relative radioactivity of each section was measured with a Tri-Carb 2910-TR liquid scintillation counter (Canberra Packard). The penetration profiles represent plots of

the measured relative specific radioactivity of the sections with background subtracted (which is proportional to the layer concentration of solute atoms, \bar{c}) versus the penetration depth, y .

III. RESULTS

As stated above, Ag diffusion in a Cu $\Sigma 5(310)$ bicrystal was measured in our previous work at low temperatures under strict C-type kinetic conditions.⁸ Hypothetically, a high density of grown-in dislocations and mosaic cell boundaries, which could potentially be present in bicrystals grown by the Bridgman method, may affect the tracer penetration. The estimates made in our previous work⁸ demonstrated that a huge density of dislocations, about 10^{15} m^{-2} , is required to violate the C-regime conditions in those measurements. Such a value can be found in a severely deformed material but not in carefully grown bicrystals.

However, we addressed this potential problem experimentally by cutting a sample near the GB and repeating the diffusion measurement. The penetration profiles measured for $^{110\text{m}}\text{Ag}$ diffusion at $T = 575$ K under C-type kinetics in samples with and without the $\Sigma 5(310)$ GB, i.e., on a single crystal in the latter case, are compared in Fig. 1. Figure 1 substantiates that the $\Sigma 5(310)$ GB does promote the Ag penetration in Cu bicrystals under the C regime and this diffusion acceleration is measurable. Therefore, the values of D_{gb} (listed in Table I) do represent the Ag GB diffusion coefficients measured in the C kinetic regime.

Figure 2 represents the $^{110\text{m}}\text{Ag}$ penetration profiles measured at higher temperatures in the intended B regime of diffusion and plotted in the coordinates of $\ln \bar{c}$ vs $y^{6/5}$. Under such conditions the GB diffusion-related parts of the penetration profiles are expected to be linear.³ The solid lines in Fig. 2 represent the corresponding fits.

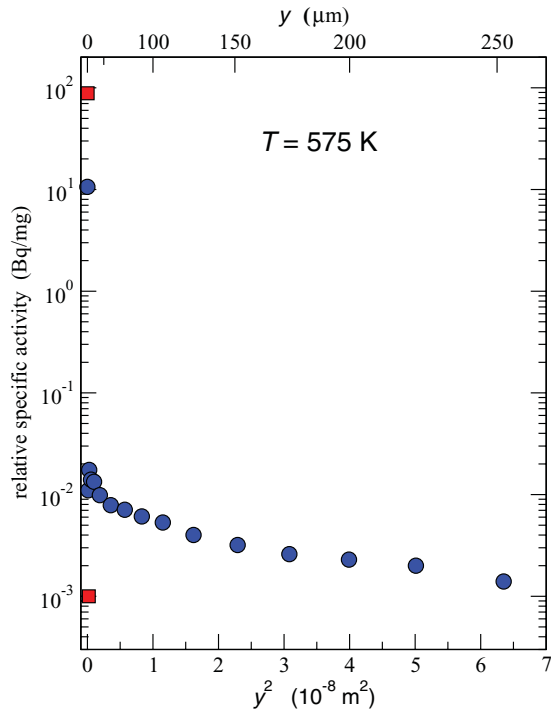


FIG. 1. (Color online) Penetration profiles of ^{110m}Ag in a Cu $\Sigma 5(310)$ bicrystal measured at $T = 575$ K for a sample which contains the grain boundary (circles) and a sample without it (squares).

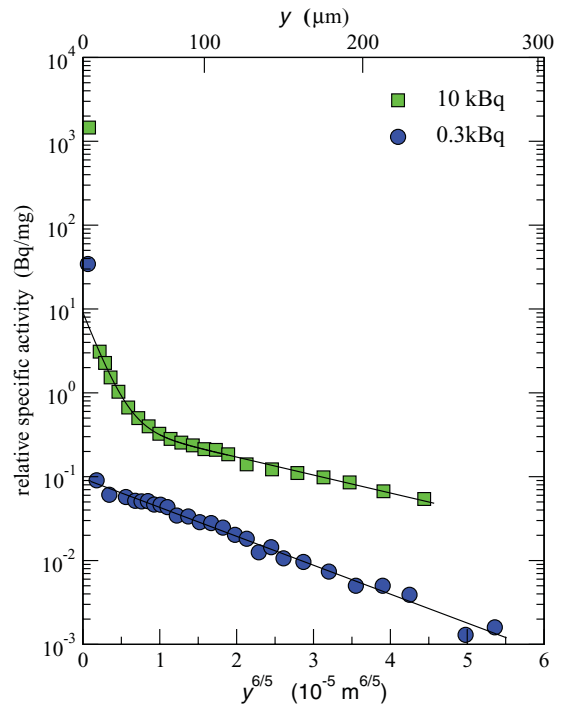


FIG. 3. (Color online) Concentration profiles measured at $T = 723$ K for Ag diffusion parallel to the tilt axis of a $\Sigma 5(310)$ bicrystal using different amounts of the applied tracer material.

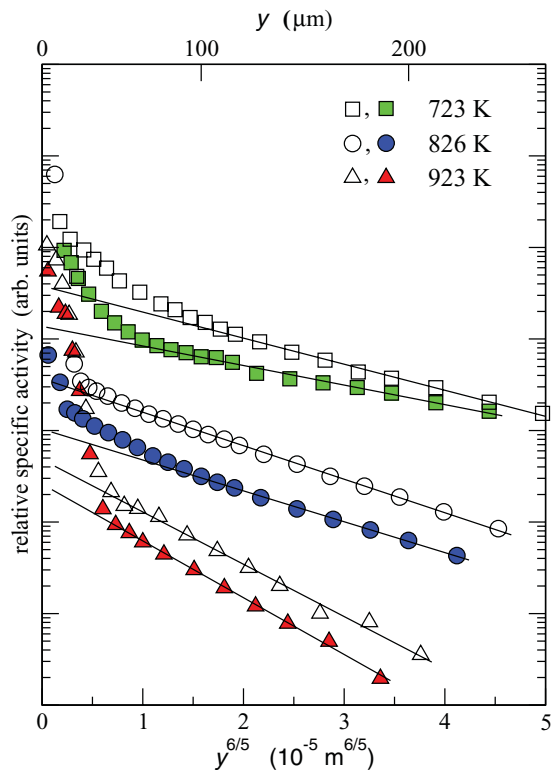


FIG. 2. (Color online) Penetration profiles of ^{110m}Ag in a Cu $\Sigma 5(310)$ bicrystal measured in the B kinetic regime of GB diffusion. Profiles are shifted vertically for convenient comparison.

A close inspection of the penetration profiles in Fig. 2 reveals that a significant nonlinearity of the GB diffusion-related parts of the penetration profiles measured in the B kinetic regime is observed at small depths. (The first near-surface points correspond to the bulk diffusion contribution, which is only significant at 923 K.) especially at moderate temperatures of 723 and 826 K (Fig. 2).

It has been shown theoretically that nonlinear GB segregation of a solute can result in a significant curvature of the corresponding penetration profiles.^{9,10} The interrelation of the nonlinear GB segregation and GB diffusion of Ag in Cu has been investigated in a number of experimental studies.^{11,12} However, those studies were carried out on polycrystalline materials, where diffusion transport occurs along an ensemble of GBs whose diffusion and segregation characteristics may differ, even dramatically (see, e.g., Ref. 13). Thus, some average characteristics were measured in those experiments, which could be the reason for the observed nonlinear penetration profiles. Moreover, the motion of a portion of the GBs during the diffusion treatment can also produce a similar curvature of the concentration profiles, and this effect was indeed encountered in our previous measurements of Ag GB diffusion in polycrystalline Cu.¹⁴

Ultimate proof of the occurrence of nonlinear segregation can be provided by a specific response of the penetration profiles upon a change of the absolute amount of diffusing solutes. Similarly to our previous study,¹⁵ two penetration profiles for ^{110m}Ag diffusion along the [001] tilt axis of the $\Sigma 5(310)$ GB at 723 K were measured (see Fig. 3). These profiles differ only by the initial amount of the ^{110m}Ag tracer

material applied to the specimen (i.e., 10 and 0.3 kBq). If a very small amount of the ^{110m}Ag tracer is applied, an almost-perfect B-type penetration profile is measured, whereas a curvature is observed for a larger amount of the initial tracer material (Fig. 3). The diffusion conditions for the case with a larger initial amount of ^{110m}Ag are listed in Table I, and the diffusion time t and the determined triple product P were 86 000 s and $2.5 \times 10^{-20} \text{ m}^3/\text{s}$ in the case of the smaller tracer amount, respectively.

The most important finding of these experiments is that the penetration profiles have to be processed until very small amounts of the solute tracer are measured. Since similar values of the triple products P were determined in the two cases, the experiment verifies that the slopes of the solid lines in Fig. 2 can be used for determination of the corresponding diffusivities. The relatively small difference in the P values measured in the two experiments may originate partially from the difference in the boundary conditions at the surface plane as indicated by Belova *et al.*¹⁶ The main advantage of the use of a larger initial amount of the applied tracer material is related to the shorter acquisition time by the nuclear detection facilities, viz., 2 vs 20 days in the case of the penetration profiles in Fig. 3.

The type of GB diffusion kinetics (and the method of analysis of the concentration profiles) is determined by the values of Le Claire's parameters, $\alpha = s\delta/2\sqrt{D_v t}$ and $\beta = P/2D_v\sqrt{D_v t}$.^{2,3,17} Here D_v is the bulk diffusion coefficient, which, for Ag in Cu, was taken from the investigation by

Barreau *et al.*:¹⁸

$$D_v = 0.61 \times 10^{-4} \exp\left\{-\frac{194.4 \text{ kJ/mol}}{RT}\right\} \text{ m}^2/\text{s}. \quad (2)$$

Following the Suzuoka solution¹⁹ for the B-regime kinetics, the value of the triple product $P = s \cdot \delta \cdot D_{\text{gb}}$ is determined from the slope of the deepest branches of the penetration profiles in Fig. 2 by the relation³

$$P = 1.308 \sqrt{\frac{D_v}{t}} \left(-\frac{\partial \ln \bar{c}}{\partial y^{6/5}}\right)^{-5/3} \quad (3)$$

at $\beta > 10^4$. The numerical factors in Eq. (3) are slightly modified at smaller values of β , Ref. 3.

Recent involved Monte Carlo calculations demonstrated that, in the case of parallel GBs, the true B-type kinetic regime holds at $\alpha < 0.1$ and the strict criterion for the C-type regime is $\alpha > 5$.²⁰ The transition regime between B and C kinetics occurs in the intermediate case, $0.1 < \alpha < 5$.

In order to process the penetration profiles measured under such conditions, the modified approach of Szabo *et al.*¹³ is used in the present paper, similarly to our recent study of Ni GB self-diffusion.²¹ The penetration profiles are replotted vs the reduced depth w , $w = y\sqrt{\beta/D_v t}$, and the averaged value of the parameter $\alpha w^{4/5}$ is determined for the GB diffusion-related part of the profile used for the fitting. Szabo *et al.* have shown¹³ that the apparent (measured) diffusivities, P^{app}

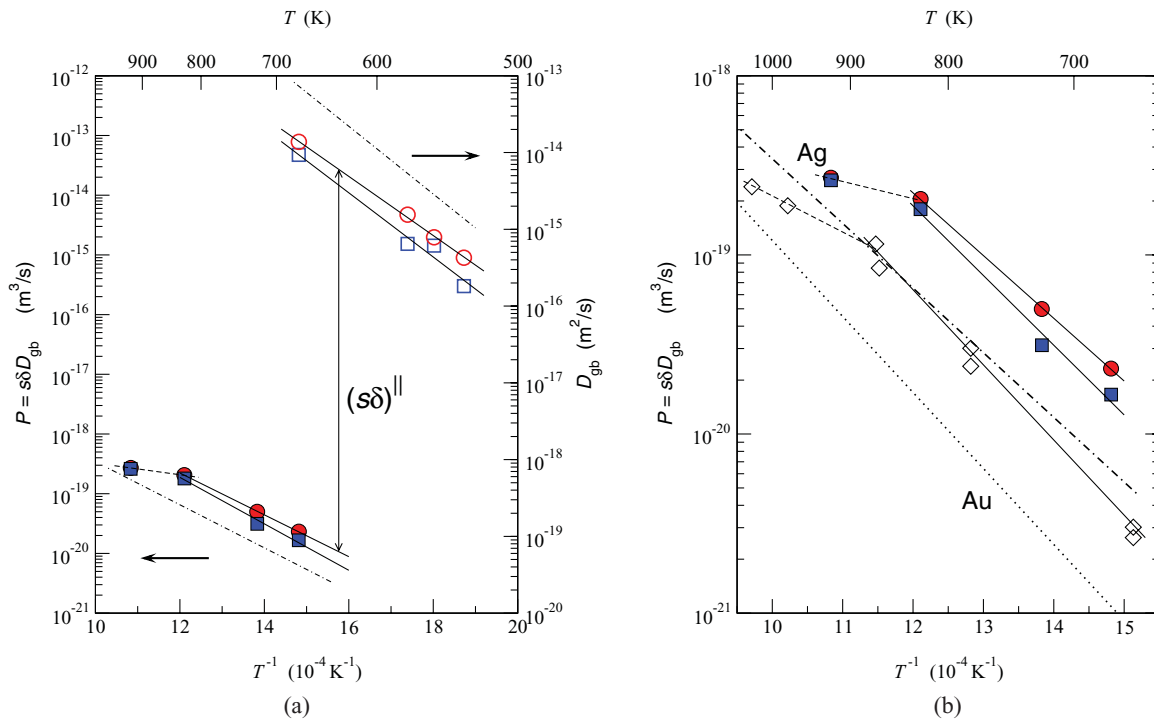


FIG. 4. (Color online) (a) Temperature dependencies of Ag GB diffusivities determined in the B (P values; filled symbols) and C (D_{gb} values; open symbols) regimes in a Cu $\Sigma 5(310)$ bicrystal. The determination of the product $s \cdot \delta$ is sketched. (b) Triple product values P for Ag diffusion in a Cu $\Sigma 5(310)$ bicrystal ($\theta = 36.3^\circ$; circles and squares) are compared to those for Au diffusion in nearly the same Cu $\Sigma 5(310)$ bicrystal ($\theta = 36.26^\circ$; diamonds).²⁴ Diffusion is measured parallel (circles) and perpendicular (squares) to the main misorientation axis of the bicrystal. GB diffusion rates of Ag (dashed-dotted lines)¹⁴ and Au (dotted line)²³ in polycrystalline Cu are shown for comparison. Note that the data points for P values at $T = 923 \text{ K}$ nearly coincide (cf. Table I).

TABLE II. Arrhenius parameters of Ag diffusion and segregation in the Cu $\Sigma 5(310)$ boundary. Values were measured for the two principal directions, parallel and perpendicular to the [001] tilt axis. Values for the segregation factors s_{\parallel} and s_{\perp} were determined assuming $\delta = 0.5$ nm.

Diffusion direction	D_{gb}		P		$s \cdot \delta$		s	
	D_{gb}^0 ($\times 10^{-6}$ m ² /s)	ΔH_{gb} (kJ/mol)	P_0 ($\times 10^{-15}$ m ³ /s)	Q_{gb} (kJ/mol)	$(s \cdot \delta)_0$ ($\times 10^{-9}$ m)	ΔH (kJ/mol)	s_0	ΔH_s (kJ/mol)
\parallel	$1.73^{+18.3}_{-1.58}$	94.8 ± 12	$3.54^{+14.3}_{-2.84}$	67.0 ± 10	$2.0^{+6.8}_{-1.6}$	-27.8 ± 10	4.0	-27.8
\perp	$4.30^{+90}_{-4.20}$	102.9 ± 18	$8.72^{+38.3}_{-7.10}$	74.5 ± 11	$2.0^{+31.5}_{-1.9}$	-28.4 ± 15	4.0	-28.4

or $D_{\text{gb}}^{\text{app}}$, determined in the transition regime between B and C kinetics are underestimated. The theoretical dependencies of the correction factors $k_{\text{B}} = P^{\text{th}}/P^{\text{app}}$ and $k_{\text{C}} = D_{\text{gb}}^{\text{th}}/D_{\text{gb}}^{\text{app}}$ on the parameter $\alpha w^{4/5}$, tabulated in Ref. 13, are used here to determine the theoretical values of the GB diffusivities, P^{th} and $D_{\text{gb}}^{\text{th}}$, respectively.

The most straightforward way to apply Eq. (1) is to perform the B- and C-type experiments at the same temperature by varying the annealing time. Unfortunately, this is practically impossible, limiting the annealing times to reasonable values for an unknown value of the product $s \cdot \delta$. In the present paper, GB diffusivities were measured over a large temperature interval and the data were fitted by corresponding Arrhenius lines. Extrapolating the P values to lower temperatures, where the D_{gb} values were measured, Eq. (1) can be applied [Fig. 4(a)].

The product $s \cdot \delta$ enters the expressions for α and β . Its value is not known *a priori*, which hinders the initial separation between the two kinetics. Therefore, an iterative strategy has been applied in the present work. The initial estimate of the product $s \cdot \delta$ was chosen from the following considerations.

(1) The effective diffusional GB width δ has been determined in a series of GB self-diffusion measurements in polycrystalline materials and a consistent value of $\delta \approx 0.5$ nm was found (see, e.g., Refs. 1, 21 and 22). As an initial guess, it was assumed that the GB width is the same for self- and solute diffusion.

(2) The segregation factors of Ag in Cu GBs measured on polycrystalline samples for random high-angle GBs¹⁴ were used as an initial estimate for the s value in the $\Sigma 5$ bicrystal.

Using this estimate, the value of α can be determined and the penetration profiles classified according to the given kinetic regime. Then the P or D_{gb} values were determined from the corresponding concentration profiles. Finally, Eq. (1) gives new estimates of the product $s \cdot \delta$ at the temperatures of the C-type measurements. The latter was approached by a linear Arrhenius dependence and used for a new iteration. The measurements at $T = 675$ and 723 K fall into the transition regime and the determined diffusivities were corrected by the method described above. These iteration steps were repeated to approach a self-consistent solution.

The final values of α , β , P , D_{gb} , and $s \cdot \delta$ for all studied temperatures are summarized in Table I. The determined values of the GB diffusivities, D_{gb} (C regime) and P (B regime), if necessary multiplied by the corresponding correction factor, are plotted on the Arrhenius coordinates in Fig. 4(a).

A strong deviation from the Arrhenius type of temperature dependence is observed for Ag diffusion in a Cu $\Sigma 5(310)$ bicrystal at $T > 826$ K for both diffusion directions, parallel and perpendicular to the tilt axis [Fig. 4(a)]. However, assuming linear dependencies of GB diffusion on the Arrhenius coordinates at 675 K $< T < 826$ K, the Arrhenius parameters for the triple product values parallel and perpendicular to the tilt axis, P_{\parallel} and P_{\perp} respectively, can be derived and they are listed in Table II. For the sake of completeness, the Arrhenius parameters determined in Ref. 8 for the GB diffusion coefficients D_{gb} are also listed in Table II.

Then, applying Eq. (1), the products of the segregation factor s and the diffusional GB width δ parallel and perpendicular to the misorientation axis are obtained (Table II). It is seen that, within the experimental uncertainties, the product $s \cdot \delta$ is isotropic.

IV. DISCUSSION

A. Temperature dependence of the GB diffusivity

Figure 4(a) suggests that the triple products $P = s \cdot \delta \cdot D_{\text{gb}}$ for Ag diffusion in the Cu $\Sigma 5(310)$ bicrystal for both principal directions (parallel and perpendicular to the tilt axis) do not follow straight lines in the Arrhenius plot over the entire temperature interval. A downward deviation is observed at $T > 826$ K. At the moment, we cannot decide between a straight Arrhenius behavior or a continuous curvature of the P values at $T > 826$ K due to the lack of a sufficient number of experimental points. The dashed line in Fig. 4 indicates the anticipated behavior of the triple product P at high temperatures. In any case, we can safely assume a decrease in the effective activation enthalpy of Ag diffusion in the Cu $\Sigma 5(310)$ GB at $T > 826$ K. We stress here that the downward deviation from the Arrhenius behavior at $T > 826$ K is observed for two data points measured independently at $T = 923 \pm 1$ K.

The next salient feature is the anisotropy of Ag GB diffusion. The GB diffusion coefficient is strongly anisotropic at low temperatures and the ratio of the diffusion coefficients parallel and perpendicular to the tilt axis, $D_{\text{gb}}^{\parallel}/D_{\text{gb}}^{\perp}$, approaches the value of 3 at $T = 534$ K. The diffusion anisotropy is still observed at $T = 723$ K, $P^{\parallel}/P^{\perp} \approx 1.6$, and it almost disappears at $T > 826$ K [see Table I and Fig. 4(a)]. These two striking features (i.e., the decrease in the effective activation enthalpy and the simultaneous disappearance of the diffusion anisotropy) indicate a structural transition of the near special $\Sigma 5(310)$ GB at temperatures of about 826 K.

A nonlinear temperature dependence of the triple product P was also observed for GB diffusion of Au in similar Cu near $\Sigma 5(310)$ bicrystals.²⁴ In Fig. 4(b) the present B-type data for Ag are compared with those for Au in a Cu $\Sigma 5(310)$ bicrystal²⁴ with nearly the same value of the main tilt angle ($\theta \approx 36.3^\circ$ in both cases and the twist component was larger in Ref. 24). (In Ref. 24, $\Phi \approx 0.5^\circ$ and the grain boundary diffusion of Au in Cu $\Sigma 5(310)$ bicrystals was measured only parallel to the [001] tilt axis.) The two temperature dependencies are very similar, suggesting a change in the effective activation enthalpy of the solute diffusion in the Cu near special $\Sigma 5$ GB at temperatures of about 850 K, i.e., at $(0.6 \div 0.7)T_m$ (T_m is the melting point of copper). Note that this feature was reported for a broad spectrum of special grain boundaries around the exact $\Sigma 5$ misorientation.²⁴ An important exemption from this rule is represented by the near $\Sigma 5$ GB with a main tilt angle $\theta = 37.57^\circ$ and a large twist component, $\Phi = 1.3^\circ$, where linear Arrhenius dependence was measured from 661 up to 1030 K.²⁴

What is the nature of the transition observed for solute diffusion in the Cu $\Sigma 5(310)$ GB? This behavior cannot be related to a relaxation of hypothetical grown-in defects caused by the bicrystal preparation, which would relax during diffusion annealing at higher temperatures. The bicrystal was grown applying a slow growth rate (12 to 16 mm/h) and a small temperature gradient across the solid/liquid interface. These conditions considerably decrease the thermal stresses and the appearance of residual defects in the GB. Moreover, the bicrystal was slowly cooled down and thus annealed at about the melting point for a reasonably long time, which guarantees a (quasi-) equilibrium GB structure.

Definitely, additional experimental efforts are required in order to differentiate between a continuous curvature and an abrupt change (kink) in the Arrhenius plot of $P(T)$. In the following, we confine the analysis to near special Cu $\Sigma 5(310)$ GB, for which detailed experimental information exists.

The continuous curvature of the Arrhenius temperature dependence of $P(T)$ at $T > T_c$ would correspond to a gradual decrease in the structural order of the grain boundaries. Alternatively, a kink in the Arrhenius plot would indicate a transition between two structural states of the GB.

The following salient features characterize the structures of the Cu near $\Sigma 5(310)$ GBs in the two temperature intervals.

(1) $T < T_c$: The crystallographic structure of grain boundaries can be substantiated for the following reasons:

- (a) pronounced anisotropy of Ag GB diffusion;
- (b) characteristic dependence of Au GB diffusion on the misorientation angles;²⁴

(c) a typical value of the effective activation enthalpy of solute GB diffusion which is equal to about 50% of the value for solute diffusion in the crystalline bulk.

(2) $T > T_c$ (but still well below T_m): The GB structure is characterized by

- (a) disappearance of the anisotropy of Ag GB diffusion;
- (b) persistence of the characteristic dependence of Au GB diffusion on the misorientation angles;²⁴

(c) decrease in the effective activation enthalpy of GB diffusion to less than 30% of the value for diffusion in the crystalline bulk, which is untypical for “normal” GB diffusion.

An idea about “special-to-general” GB phase transition at a certain temperature T_c was elaborated in investigations

on thermodynamic and kinetic properties of GBs.^{25–27} The temperature T_c was related to the magnitude of the deviation in orientation from the special high coincidence GB, and with increasing deviation from the ideal low- Σ GB, T_c was predicted to decrease.²⁷ The thermodynamic nature of this transition is not well established yet.²⁸

Earlier molecular dynamics (MD) studies²⁹ indicated a “solid-like” state of a $\Sigma 5(310)$ GB almost up to the melting point with a temperature-induced disorder due to an increasing point defect concentration in the interface. Alternatively, a more recent MD investigation³⁰ predicts a “liquid-like” state of high-angle grain boundaries in Pd at $T > T_c$ with an “amorphous” structure and isotropic diffusivity in the interface. The transition temperature T_c was predicted to decrease with increasing GB energy, which was related to an increased short-range disorder of the GB structure.³⁰ For the presently studied $\Sigma 5$ GB, the transition from solid-like to liquid-like diffusion was predicted to occur at roughly $0.65T_m$,³⁰ which is in nice agreement with the present findings. However, more recent simulations^{31,32} predict GB premelting and formation of a liquid-like layer in high-angle GBs in Cu at about 10 K below the melting point, which is far beyond the temperature interval studied here.

We conclude that there still exists no adequate theory which would unambiguously explain all experimental facts. A “phase transition” of the GB structure around T_c does follow from the experimental data, but the nature of the high-temperature ($T > T_c$) GB structure—e.g., liquid-like or solid-like—is still to be elucidated. As follows from Fig. 4(b), the values of the triple product P for Ag and Au diffusion in near special Cu $\Sigma 5(310)$ bicrystals are larger than the corresponding values for diffusion along general (random) high-angle GBs in polycrystalline copper and approach them with increasing temperature. Moreover, almost-perfect Arrhenius-type temperature dependencies are observed for both Ag and Au diffusion in polycrystalline Cu in the true B kinetic regime, while nonlinearities are obvious for near special $\Sigma 5(310)$ bicrystals.

Residual impurities could potentially represent a serious issue for experimental studies. The present and literature^{14,24} data refer to a high-purity copper material of 99.9998 wt% nominal purity. The concentration of residual sulfur was found to be about 0.1 ppm in this material.³³ The impurity content in the Cu bicrystals has to be at least on a similar level due to the “zone remelting” purification effect during bicrystal production. Such purity levels are probably sufficient to represent the “true” GB properties of both bicrystalline and polycrystalline copper materials. Careful measurements on selected alloy systems can help to clarify this problem.

An attempt to generalize the high-temperature structure of a near special GB just in terms of an amorphous-like structure can be incomplete, since the localization of the specific free volume in the interface could also play an important role. For example, recent studies indicate the existence of internal interfaces in bulk metallic glasses with a localized additional free volume³⁴ and even significantly enhanced associated diffusivities.³⁵

Recent atomistic simulation³⁶ of $\Sigma 5(210)$ and $\Sigma 41(540)$ GBs indicated a structure transition at about 500 to 600 K related to the disappearance of the “open channels” along the [001] tilt axis. The GB transition was accompanied by a change

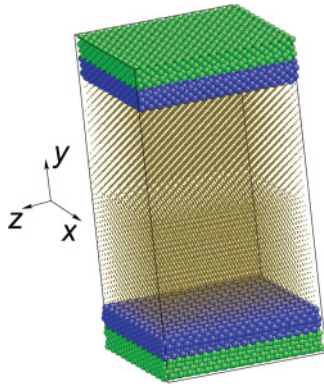


FIG. 5. (Color online) Simulation block used in the present calculations. Fixed (green), buffer (blue), and free (gold) atoms are distinguished. The grain boundary lies in the xz plane and the $[001]$ tilt axis is parallel to the z axis.

in the GB width.³⁶ The open channels are characteristic for the low-temperature structure of these interfaces.³⁷

We have performed a small-scale MD simulation of a Cu $\Sigma 5(310)$ GB using the LAMMPS software^{38,39} and applying the embedded-atom method potentials developed by Mishin *et al.*⁴⁰ A $\Sigma 5(310)$ GB was introduced in a simulation box of $6.9 \times 12.7 \times 6.6 \text{ nm}^3$ containing 47 520 atoms. The zero-temperature equilibrium structure was found by energy minimization and then the given MD runs were performed. The NVT ensemble (with the number of atoms N , the total

volume V , and the temperature T kept constant) was employed with fixed boundary conditions perpendicular to the boundary plane and periodic conditions parallel to the boundary. The simulation block is shown in Fig. 5, where fixed, buffer, and free Cu atoms are distinguished by coloring. The radius of the free atoms is diminished for better visualization.

Before a given MD run, the simulation block and the atomic coordinates, equilibrated previously at $T = 0 \text{ K}$, were rescaled to account for the thermal expansion. After a short equilibration, for 100 ps, the atomic trajectories were followed over 10 ns.

Figures 6(a)–6(f) show atomic structures observed for the Cu $\Sigma 5(310)$ GB at selected temperatures from 200 to 1300 K. Open channels are clearly present in the Cu $\Sigma 5(310)$ GB at $T \leq 800 \text{ K}$ [Fig. 6(a)]. These open channels are hardly distinguishable at $T = 900 \text{ K}$ [Fig. 6(d)] and they disappear completely at $T = 1000 \text{ K}$ [Fig. 6(e)]. For the given MD runs, significant amorphization and thickening of the GB are observed near the melting point at $T = 1300 \text{ K}$ [Fig. 6(f)].

We propose that the disordering of the atomic structure related to the disappearance of the open channels probably induces a characteristic change in the GB structure and kinetic properties. This phenomenon may explain the experimentally observed transition in the diffusion behavior. Qualitative agreement between the experimental data and the simulation results can safely be stated, although detailed atomistic simulations are required in order to determine the nature and the characteristics of the structural transition.

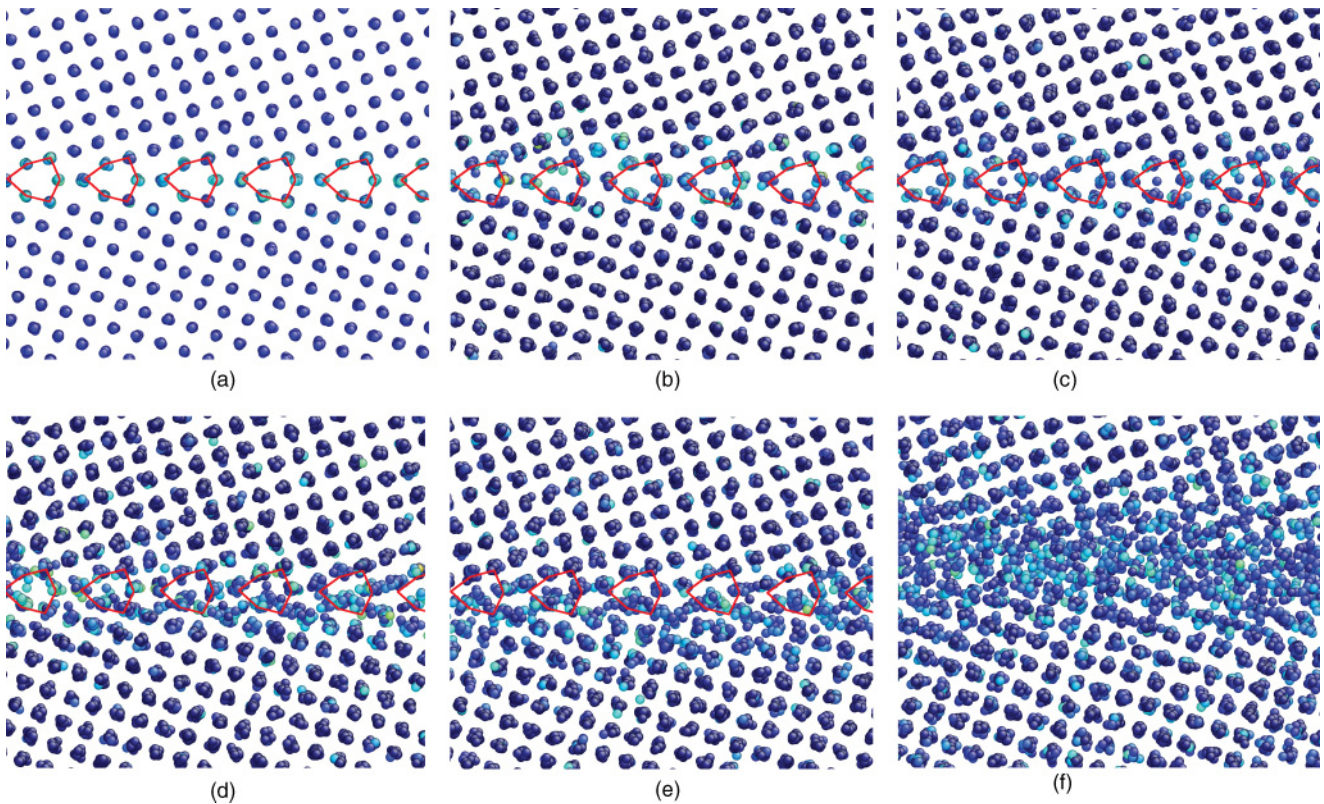


FIG. 6. (Color online) Atomic structure [projection along the tilt (001) axis] of the Cu $\Sigma 5(310)$ grain boundary after a 10-ns MD run at 200 K (a), 700 K (b), 800 K (c), 900 K (d), 1000 K (e), and 1300 K (f). The structure elements representing the “open channels” in the structure relaxed at $T = 0 \text{ K}$ are sketched. Atoms are color-coded according to their central symmetry parameter.⁴¹

Cu self-diffusion in $\Sigma 5(310)$ and $\Sigma 5(210)$ GBs was simulated by Suzuki and Mishin.³² Diffusion was isotropic in the $\Sigma 5(210)$ GB at $T > 700$ K, and anisotropy of Cu self-diffusion in the $\Sigma 5(310)$ GB was recorded below 900 K.³² A striking feature is that the diffusion coefficients of the $\Sigma 5(310)$ and $\Sigma 5(210)$ GBs are almost identical at $T > 900$ K (see Fig. 4 in Ref. 32). An open question is whether the GB self-diffusion in the $\Sigma 5(210)$ GB is anisotropic at $T < 500$ K, i.e., below the temperature of the structure transition reported in Ref. 36.

B. Grain boundary segregation of Ag

In Fig. 4(a), the rates of Ag GB diffusion in Cu $\Sigma 5(310)$ bicrystals (present data) and in high-purity polycrystalline Cu (measured previously by us)¹⁴ are compared. This comparison suggests that Ag diffuses slowly in the near special $\Sigma 5(310)$ boundary with respect to general (random) high-angle GBs in polycrystalline copper, $D_{\text{gb}}^{\Sigma 5(310)} < D_{\text{gb}}^{\text{rand}}$, while the opposite trend is established for the triple product values, $P^{\Sigma 5(310)} > P^{\text{rand}}$. Since the GB width δ is virtually the same for random and special high-angle GBs, these relations suggest that Ag segregates more strongly to near special $\Sigma 5(310)$ GBs than to general (random) high-angle grain boundaries in polycrystalline copper.

This observation cannot definitely be generalized for *all* low- Σ GBs in Cu. For example, the GB diffusivities P measured for incoherent twin boundaries in Cu are smaller

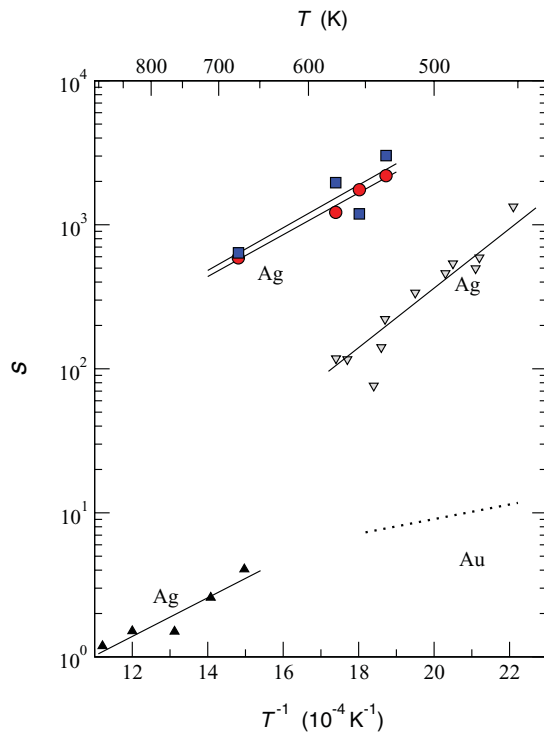


FIG. 7. (Color online) Temperature dependences of the segregation coefficient s of Ag in the Cu $\Sigma 5(310)$ boundary measured via GB diffusion parallel (circles) and perpendicular (squares) to the tilt axis. For comparison, GB segregation factors measured in *polycrystalline* Cu for Ag (downward triangles),¹⁴ Au (dotted line),²³ and Ag in Cu-0.2 at% Ag alloy (upward triangles)⁴⁴ are shown.

than the P values determined for general high-angle GBs in polycrystalline material (see Fig. 8). Note that due to the structural multiplicity of the $\Sigma 3$ incoherent twin boundary in copper, two different values, slower (downward triangles) and faster (upward triangles) ones, were measured in Ref. 42 for Au as well as in Ref. 43 for Ag (Fig. 8). For further details see Ref. 42.

Atomistic simulation of $\Sigma 5(210)$ GB in Cu and Cu-Ag alloys has shown that a notable variation in the GB structure width occurs only at temperatures close to the melting point.³¹ These findings are also supported by the present simulation of the Cu $\Sigma 5(310)$ GB (Fig. 6). Accordingly, we assume that the diffusion GB width δ is approximately constant and does not depend on the temperature and diffusion direction in the temperature interval studied, $534 \text{ K} < T < 923 \text{ K}$. In the following, the estimate $\delta = 0.5 \text{ nm}$ is used. Then the segregation factors s can be determined (Table II). In Fig. 7, the temperature dependencies of the derived segregation coefficients are compared with the previously measured GB segregation coefficients of Ag in polycrystalline Cu¹⁴ and Cu-0.2 at% Ag alloy.⁴⁴

The stronger segregation of Ag to the Cu $\Sigma 5(310)$ GB compared with that to random high-angle GBs in polycrystalline copper is obvious. Simultaneously, the segregation enthalpies are not very different. This fact is likely related

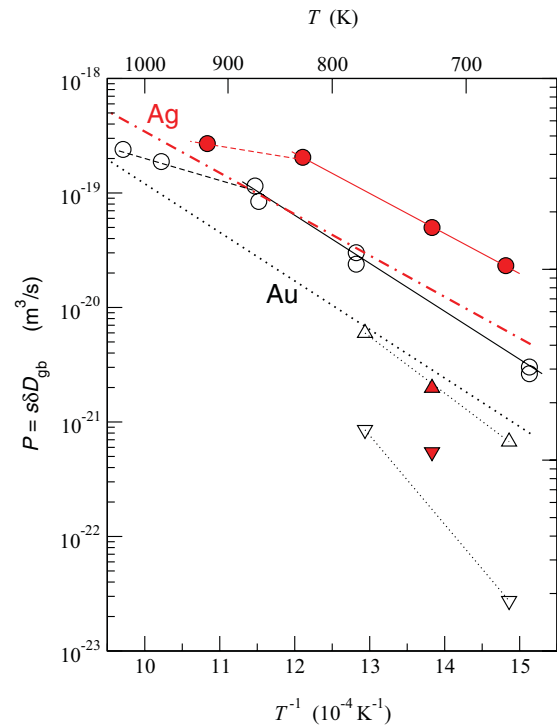


FIG. 8. (Color online) Diffusion of Ag [filled symbols: in $\Sigma 5(310)$ (present work) and in $\Sigma 3$ ⁴³] and Au [open symbols: in $\Sigma 5(310)$ ²⁴ and in $\Sigma 3$ ⁴²] in low- Σ GBs in Cu in comparison to that along the general high-angle GBs in polycrystalline material (dashed-dotted¹⁴ and dotted²³ lines, respectively). Diffusion was measured along the main tilt axes of $\Sigma 5(310)$ (circles) and incoherent $\Sigma 3$ (triangles) grain boundaries. Two contributions, slower (downward triangles) and faster (upward triangles) ones, were determined for the incoherent twin boundaries; see text.

to the higher density of parallel open channels along the [001] misorientation axis in the low-temperature structure of the $\Sigma 5(310)$ GB in Cu, which offer attractive sites for segregation of oversized Ag atoms (see Fig. 6). Note that these parallel open channels characterize the low- Σ CSL tilt GBs, whose fraction in real polycrystals is small.

Practically the same segregation factors are found from independent measurements of Ag diffusion along and perpendicular to the tilt axis of the Cu $\Sigma 5(310)$ GB (Fig. 7), despite the distinct anisotropy of GB diffusion (Fig. 4). This fact supports the correctness of the present estimates: the segregation factor in the dilute limit (as is the case for the present radiotracer measurements) accounts for the thermodynamic equilibrium for solute atoms between the boundary plane and the crystalline bulk adjacent to the GB. This equilibrium is approached via the atomic jumps perpendicular to the boundary plane and it should not be affected by the direction of the tracer gradient along the boundary.

In Fig. 7, the GB segregation factors for Ag and Au in Cu are also compared. It is interesting that the relation $p^{\Sigma 5(310)} > p^{\text{rand}}$ is valid for both strongly (Ag) and slightly (Au) segregating solutes in Cu (cf. Figs. 4 and 7). This fact indicates that the structure of Cu $\Sigma 5$ GBs probably cannot be considered as an amorphous layer, at least at temperatures below 850 K, as follows from the present simulation (Fig. 6).

V. SUMMARY

In the present work, GB diffusion of Ag in Cu $\Sigma 5(310)$ bicrystals is measured under B and C kinetic regime conditions

using the radiotracer technique. The observed anisotropy of diffusion and its temperature dependence are analyzed in relation to the atomistic mechanism of solute GB diffusion with respect to the GB structure.

The temperature dependence of Ag GB diffusion in Cu $\Sigma 5(310)$ bicrystals is found to be nonlinear, with a downward deviation from the anticipated Arrhenius dependence above a certain temperature, $T_c \approx 820$ K. The change in the effective activation enthalpy of diffusion is accompanied by the disappearance of the diffusion anisotropy, indicating a structural transition of the $\Sigma 5$ boundary at $T = T_c$. This fact suggests, at least, that the increasing atomic disordering affects the “open channels” in the $\Sigma 5$ boundaries at $T > T_c$.

A stronger segregation of Ag to the Cu $\Sigma 5(310)$ boundary than to general (random) high-angle GBs in polycrystalline copper is found. Simultaneously, the opposite trend is observed for the corresponding GB diffusion coefficients: the D_{gb} for Ag in near special $\Sigma 5(310)$ GB is smaller than that in general high-angle GBs.

ACKNOWLEDGMENTS

The authors would like to thank T. Frolov and Y. Mishin (George Mason University, Fairfax, Virginia) for stimulating discussions and sharing of their simulation results³⁶ prior to publication. We are grateful to P. Skyba for technical assistance with the radiotracer measurements. The financial support of the Deutsche Forschungsgemeinschaft (Grant No. Di 1419/3-1) is acknowledged. Tracer activation at research reactor GKSS, Geesthacht, Germany, is acknowledged.

*divin@uni-muenster.de

¹S. V. Divinski and Chr. Herzig, *J. Mater. Sci.* **43**, 3900 (2008).

²L. G. Harrison, *Trans. Faraday Soc.* **57**, 1191 (1961).

³I. Kaur, Y. Mishin, and W. Gust, *Fundamentals of Grain and Interface Boundary Diffusion* (Wiley, Chichester, UK, 1995).

⁴S. V. Divinski and B. S. Bokstein, *Defect Diffus. Forum* **309-310**, 1 (2011).

⁵J. R. Trelewicz and C. A. Schuh, *Phys. Rev. B* **79**, 094112 (2009).

⁶I. Kaur, L. Kozma, and W. Gust, *Handbook of Grain and Interphase Boundary Diffusion Data* (Ziegler, Stuttgart, 1989).

⁷Q. Ma and R. W. Balluffi, *Acta Metall. Mater.* **41**, 133 (1993).

⁸H. Edelhoff, S. I. Prokofjev, and S. V. Divinski, *Scripta Mater.* **64**, 374 (2011).

⁹B. S. Bokstein, V. E. Fradkov, and D. L. Beke, *Philos. Mag. A* **65**, 277 (1992).

¹⁰Y. M. Mishin and Chr. Herzig, *J. Appl. Phys.* **73**, 8206 (1993).

¹¹J. Bernardini, Zs. Tökei, and D. L. Beke, *Philos. Mag. A* **73**, 237 (1996).

¹²B. Bokstein, A. S. Ostrovsky, and J. Bernardini, *Mater. Sci. Forum.* **294-296**, 553 (1999).

¹³I. A. Szabó, D. L. Beke, and F. J. Kedves, *Philos. Mag. A* **62**, 227 (1990).

¹⁴S. V. Divinski, M. Lohmann, and Chr. Herzig, *Acta Mater.* **49**, 249 (2001).

¹⁵S. V. Divinski, M. Lohmann, S. I. Prokofjev, and Chr. Herzig, *Z. Metallkd.* **96**, 1181 (2005).

¹⁶I. V. Belova, G. E. Murch, and Th. Fiedler, *Defect Diffus. Forum* **309-310**, 9 (2011).

¹⁷A. D. Le Claire, *Br. J. Appl. Phys.* **14**, 351 (1963).

¹⁸G. Barreau, G. Brunel, G. Cizeron, and P. Lacombe, *C.R. Acad. Sci. (Paris) C* **270**, 516 (1970).

¹⁹T. Suzuoka, *J. Phys. Soc. Jpn.* **19**, 839 (1964).

²⁰I. V. Belova, G. E. Murch, and Th. Fiedler, *Defect Diffus. Forum* **297-301**, 1226 (2010).

²¹S. V. Divinski, G. Reglitz, and G. Wilde, *Acta Mater.* **58**, 386 (2010).

²²J. Sommer and Chr. Herzig, *J. Appl. Phys.* **72**, 2758 (1992).

²³T. Surholt, Y. M. Mishin, and Chr. Herzig, *Phys. Rev. B* **50**, 3577 (1994).

²⁴E. Budke, T. Surholt, S. I. Prokofjev, L. S. Shvindlerman, and Chr. Herzig, *Acta Mater.* **47**, 385 (1999).

²⁵A. N. Aleshin, S. I. Prokofjev, and L. S. Shvindlerman, *Scripta Metall.* **19**, 1135 (1985).

²⁶B. B. Straumal, L. M. Klinger, and L. S. Shvindlerman, *Acta Metall.* **32**, 1355 (1984).

²⁷E. L. Maksimova, E. I. Rabkin, L. S. Shvindlerman, and B. B. Straumal, *Acta Metall.* **37**, 1995 (1989).

²⁸Y. Mishin, M. Asta, and J. Li, *Acta Mater.* **58**, 1117 (2010).

²⁹G. Ciccotti, M. Guillope, and V. Pontikis, *Phys. Rev. B* **27**, 5576 (1983).

- ³⁰P. Keblinski, D. Wolf, S. R. Phillpot, and H. Gleiter, *Philos. Mag. A* **79**, 2735 (1999).
- ³¹P. L. Williams and Y. Mishin, *Acta Mater.* **57**, 3786 (2009).
- ³²A. Suzuki and Y. Mishin, *J. Mater. Sci.* **40**, 3155 (2005).
- ³³T. Surholt and Chr. Herzig, *Acta Mater.* **45**, 3817 (1997).
- ³⁴D. Söpu, K. Albe, Y. Ritter, and H. Gleiter, *Appl. Phys. Lett.* **94**, 191911 (2009).
- ³⁵J. Bokeloh, S. V. Divinski, G. Replitz, and G. Wilde, *Phys. Rev. Lett.* **107**, 235503 (2012).
- ³⁶T. Frolov and Y. Mishin, unpublished (2011).
- ³⁷M. R. Sørensen, Y. Mishin, and A. F. Voter, *Phys. Rev. B* **62**, 3658 (2000).
- ³⁸[<http://lammmps.sandia.gov/cite.html>].
- ³⁹S. J. Plimpton, *J. Comput. Phys.* **117**, 1 (1995).
- ⁴⁰Y. Mishin, M. J. Mehl, D. A. Papaconstantopoulos, A. F. Voter, and J. D. Kress, *Phys. Rev. B* **63**, 224106 (2001).
- ⁴¹C. L. Kelchner, S. J. Plimpton, and J. C. Hamilton, *Phys. Rev. B* **58**, 11085 (1998).
- ⁴²E. Rabkin, C. Minkwitz, Chr. Herzig, and L. Klinger, *Philos. Mag. Lett.* **79**, 409 (1999).
- ⁴³I. Binkowski, Diploma thesis, Münster University (2012).
- ⁴⁴S. Divinski, M. Lohmann, and Chr. Herzig, *Interface Sci.* **11**, 21 (2003).